OXFORD GENETICS

GENETICS, 2022, 220(1), iyab186
https://doi.org/10.1093/genetics/iyab186
Advance Access Publication Date: 2 November 2021
Investigation

Neuronal KGB-1 JNK MAPK signaling regulates the dauer developmental decision in response to environmental stress in *Caenorhabditis elegans*

Deepshikha Dogra ,[1,2] Warakorn Kulalert,[2,†] Frank C. Schroeder,[3,4] and Dennis H. Kim[1,*]

[1]Division of Infectious Diseases, Department of Pediatrics, Boston Children's Hospital and Harvard Medical School, Boston, MA 02115, USA,
[2]Department of Biology, Massachusetts Institute of Technology, Cambridge, MA 02139, USA,
[3]Boyce Thompson Institute, Ithaca, NY 14853, USA, and
[4]Department of Chemistry and Chemical Biology, Cornell University, Ithaca, NY 14853, USA

*Corresponding author: Division of Infectious Diseases, Boston Children's Hospital, 300 Longwood Ave, Boston, MA 02115, USA. Email: dennis.kim@childrens.harvard.edu
†Present address: Metaorganism Immunity Section, Laboratory of Host Immunity and Microbiome, National Institute of Allergy and Infectious Diseases, National Institute of Health, Bethesda, MD 20892, USA.

Abstract

In response to stressful growth conditions of high population density, food scarcity, and elevated temperature, young larvae of nematode *Caenorhabditis elegans* can enter a developmentally arrested stage called dauer that is characterized by dramatic anatomic and metabolic remodeling. Genetic analysis of dauer formation of *C. elegans* has served as an experimental paradigm for the identification and characterization of conserved neuroendocrine signaling pathways. Here, we report the identification and characterization of a conserved c-Jun N-terminal Kinase-like mitogen-activated protein kinase (MAPK) pathway that is required for dauer formation in response to environmental stressors. We observed that loss-of-function mutations in the MLK-1-MEK-1-KGB-1 MAPK pathway suppress dauer entry. A loss-of-function mutation in the VHP-1 MAPK phosphatase, a negative regulator of KGB-1 signaling, results in constitutive dauer formation, which is dependent on the presence of dauer pheromone but independent of diminished food levels or elevated temperatures. Our data suggest that the KGB-1 pathway acts in the sensory neurons, in parallel to established insulin and TGF-β signaling pathways, to transduce the dauer-inducing environmental cues of diminished food levels and elevated temperature.

Keywords: *Caenorhabditis elegans*; dauer decision; KGB-1 pathway; JNK MAPK; sensory neurons

Introduction

Caenorhabditis elegans can enter an alternative developmental diapause state, known as dauer, in response to unfavorable environmental conditions—specifically increased population density, scarcity of bacterial food, and elevated temperature (Golden and Riddle 1982, 1984a, 1984b, 1984c). The dauer state is characterized by increased stress resistance and dramatic remodeling of anatomy and metabolism (Cassada and Russell 1975). The genetic analysis of dauer formation has served as an experimental paradigm for understanding how neuroendocrine signaling through conserved components such as the insulin, TGF-β, and nuclear hormone receptor pathways control organismal physiology and modulate developmental plasticity (Riddle and Albert 1997; Hu 2007; Fielenbach and Antebi 2008; Baugh and Hu 2020).

Recent studies have defined the molecular basis for how *C. elegans* responds to increased population density through pheromone signaling. Dauer pheromone has been characterized as a mixture of ascarosides, several structurally related derivatives of the dideoxysugar ascarylose (Butcher *et al.* 2007), which act on diverse families of G-protein-coupled membrane receptors (GPCRs). Receptors encoded by *srbc-64* and *srbc-66* are involved in the perception of ascarosides ascr#1, ascr#2, and ascr#3, with probable role of additional GPCRs as the double mutant *srbc-64; srbc-66* still forms dauer at high concentrations of these ascarosides (Kim *et al.* 2009). McGrath *et al.* (2011) identified two predicted GPCRs, *srg-36* and *srg-37*, as ascr#5-specific receptors. Two additional receptors, DAF-37 and DAF-38, respond to ascr#2, ascr#3, and ascr#5 (Park *et al.* 2012). Pheromone signaling also modulates expression of DAF-7 (TGF-β ligand) and insulin ligands (Ren *et al.* 1996; Schackwitz *et al.* 1996; Li *et al.* 2003), linking the activity of pheromone to canonical signaling pathways involved in the control of the dauer developmental decision.

In contrast, the mechanisms by which diminished levels of high-quality bacterial food or temperature can modulate the dauer decision remain less well understood. Food signal was first described as a compound present in bacterial extract that can inhibit dauer formation and initiate dauer recovery (Golden and Riddle 1982, 1984a). Bacterial fatty acids have been implicated in promoting dauer recovery (Kaul *et al.* 2014). Of note, recent studies have shown a role of Rictor/TORC2 and CaMKI in regulating the expression of TGF-β ligand and insulin-like proteins in

Received: July 07, 2021. **Accepted:** October 15, 2021

response to food signals in dauer entry (Neal *et al.* 2015; O'Donnell *et al.* 2018).

We previously described a genetic strategy to identify novel genes involved in dauer formation by undertaking a screen for suppressors of the *daf-28(sa191)* mutation (Kulalert and Kim 2013; Kulalert *et al.* 2017), which confers constitutive entry into dauer diapause (Malone *et al.* 1996; Li *et al.* 2003). Here, we have identified and characterized a c-Jun N-terminal Kinase (JNK)-like mitogen-activated protein kinase (MAPK) KGB-1 pathway that functions in the sensory neurons to promote dauer formation. We characterize the effect of loss of the KGB-1 pathway, as well as its hyperactivation in a VHP-1 MAPK phosphatase mutant, on the regulation of the dauer developmental decision. Our data suggest a role for KGB-1 signaling in transducing diminished bacterial food and elevated temperature cues, which are integrated with pheromone signaling to promote entry into dauer diapause.

Materials and methods

Strains

All *C. elegans* strains used in this study were maintained as previously described (Brenner 1974). The temperature sensitive strains were maintained at 16°C and all other strains were incubated at 20°C. The following is a complete list of all the strains used in this study:

Strain	Genotype
N2	Wild-type
KU21	*kgb-1(km21)*
KB3	*kgb-1(um3)*
ZD2520	*mek-1(qd375)*
FK171	*mek-1(ks54)*
ZD1645	*mlk-1(qd318)*
ZD108	*mlk-1(km19)*
FXO1729	*shc-1(tm1729)*
VC822	*kgb-2(gk361)*
VC8	*jnk-1(gk7)*
BS3383	*pmk-3(ok169)*
JT366	*vhp-1(sa366)*
ZD2350	*vhp-1(sa366);kgb-1(km21)*
ZD2638	*vhp-1(sa366);mek-1(qd375)*
ZD110	*vhp-1(km20)/mIn1*
ZD2113	*mek-1(qd375);qdEx197[mek-1(+)]*
ZD2110	*mek-1(qd375);qdEx198[mek-1(+)]*
ZD2324	*mek-1(qd375);qdEx199[mek-1(+)]*
ZD2351	*mek-(qd375);qdEx187[rab-3p::mek-1::F2A::mCherry::unc-54 3'UTR]*
ZD2508	*mek-(qd375);qdEx191[rab-3p::mek-1::F2A::mCherry::unc-54 3'UTR]*
ZD2325	*mek-1(qd375);qdEx200[elt-2p::mek-1::F2A::mCherry::unc-54 3'UTR]*
ZD2326	*mek-1(qd375);qdEx201[elt-2p::mek-1::F2A::mCherry::unc-54 3'UTR]*
ZD2543	*mek-1(qd375);qdEx202[elt-2p::mek-1::F2A::mCherry::unc-54 3'UTR]*
ZD2506	*mek-1(qd375);qdEx189[myo-3p::mek-1::F2A::mCherry::unc-54 3'UTR]*
ZD2507	*mek-1(qd375);qdEx190[myo-3p::mek-1::F2A::mCherry::unc-54 3'UTR]*
ZD2513	*mek-1(qd375);qdEx192[myo-3p::mek-1::F2A::mCherry::unc-54 3'UTR]*
ZD2569	*mek-1(qd375);qdEx194[bbs-1p::mek-1::F2A::mCherry::unc-54 3'UTR]*
ZD2570	*mek-1(qd375);qdEx195[bbs-1p::mek-1::F2A::mCherry::unc-54 3'UTR]*
ZD2571	*mek-1(qd375);qdEx196[bbs-1p::mek-1::F2A::mCherry::unc-54 3'UTR]*
CF1038	*daf-16(mu86)*
ZD2518	*daf-16(mu86);vhp-1(sa366)*
DR20	*daf-12(m20)*
ZD2567	*daf-12(m20);vhp-1(sa366)*
CB1376	*daf-3(e1376)*
ZD2639	*daf-3(e1376);vhp-1(sa366)*
TY3856	*cuIs5[myo2C::GFP+pRF4(rol-6(su1006))]*
TY3862	*cuIs5[myo2C::GFP+pRF4(rol-6(su1006))]; daf-7(e1372)*
ZD2640	*cuIs5[myo2C::GFP+pRF4(rol-6(su1006))]; vhp-1(sa366)*

Dauer formation assays

The dauer assays, unless otherwise mentioned, were performed broadly as described (Neal *et al.* 2013), using the following-indicated pheromone mix, food sources, and temperatures. One hundred microliters of pheromone mix (containing ascarosides ascr#2, ascr#3, ascr#5, and ascr#8 each at a concentration of 20 μM in 10% ethanol) was added to 3.5 cm plates (volume ~3 ml) made with Noble agar and without peptone, resulting in an effective plate concentration of 0.67 μM for each ascaroside. The plates were seeded with 20 μl of either concentrated heat-killed (60 mg/ml) or live (70 mg/ml) *Escherichia coli* strain OP50. Three to five gravid animals per individual plate were allowed to lay eggs for 3 h at assay temperature (25°C). The numbers of dauer and non-dauer animals were scored 72 h (heat-killed food) or 64 h (live food) post egg-lay midpoint. The assays with incubation at lower temperatures only differed in their length of incubation, the numbers of dauer and non-dauer animals were scored 96 h (20°C) and 120 h (16°C) post egg-lay midpoint.

Partial dauer characterization

Partial dauers are animals that possess some but not all characteristics of dauer. These dauer-like animals have a refractile intestine resembling a dauer and radial constriction of the body but not of the pharynx. Pumping is not completely halted, and fat stores are not accumulated but the cuticle structure resembles dauer alae (Vowels and Thomas 1992; Larsen *et al.* 1995; Ogg *et al.* 1997). We identified partial dauers morphologically and we used treatment with 1% SDS for definitive characterization. Previous studies have reported that partial dauers can survive SDS treatment longer than non-dauer animals but not as long as dauers (Nika *et al.* 2016). While non-dauer larvae and adult *C. elegans* animals are only able to survive in SDS for less than 10 min, dauers can easily survive longer than 60 min. Partial dauers on the other hand are able to survive for approximately 18–20 min, making their survival time much higher than the non-dauer animals but less than dauers.

Cloning and generation of transgenic lines

For the genomic rescue construct, the endogenous promoter of *mek-1* (4.2 kb upstream), along with the entire gene and 3′ UTR (1 kb downstream) sequence were amplified from genomic DNA using forward primer 5′-GGCATAAAACATGCTGAAAAATAAATTC-3′ and reverse primer 5′-CCACGCCTAGACTGGTTTATC-3′. This PCR product was cloned into pUC19 backbone using NEBuilder HiFi DNA Assembly (New England Biolabs, Ipswich, MA, USA). The assembled plasmid was microinjected at 25 ng/μl concentration, along with

ofm-1p::gfp as a co-injection marker at 50 ng/µl for endogenous *mek-1* rescue in the *mek-1* loss-of-function mutant background.

For tissue-specific expression constructs, MEK-1 cDNA (K08A8.1a.1) was amplified from N2 cDNA library using PCR. N2 cDNA library was created in lab using RNA isolation and reverse transcription. The cDNA expression was driven by various tissue-specific promoters viz. *elt-2p* (intestine-specific expression), *myo-3p* (body wall muscle-specific expression), *rab-3p* (pan-neuronal expression) and *bbs-1p* (pan-ciliated neuron-specific expression). The promoters along with the cDNA, F2A self-cleaving peptide, and mCherry sequence were all cloned into pPD95.75 plasmid backbone using NEBuilder HiFi DNA Assembly. The mCherry sequence was used to help confirm the expression of MEK-1 in the specific tissue, and the F2A self-cleaving peptide sequence ensured that MEK-1 and mCherry do not form a fusion protein.

The assembled plasmid for body-wall muscle-specific expression was microinjected at 25 ng/µl concentration, along with *ofm-1p::gfp* as a co-injection marker at 50 ng/µl for tissue-specific rescue of *mek-1* in the *mek-1* loss-of-function mutant background. The remaining assembled plasmids were microinjected at 5 ng/µl concentration (due to toxicity issues at higher concentration), along with *ofm-1p::gfp* as a co-injection marker at 100 ng/µl for tissue-specific rescue of *mek-1* in the *mek-1* loss-of-function mutant background.

Imaging

For measurement of *culs5* GFP in the pharynx, animals were egg laid in the pheromone assay as described above and 24 h post egg-lay midpoint, the animals were mounted with 1 mM sodium azide onto slides with a 2% agarose pad. Slides were viewed using Zeiss AxioImager Z1 fluorescence microscope primarily with 20× objective. Fluorescence signals were recorded with a charge-coupled device camera (AxioCam) using constant exposure time without saturation. For quantification, maximum intensity values of GFP within the pharynx were calculated using FIJI software (Schindelin *et al.* 2012; Fiji, RRID: SCR_002285).

Statistical analysis

All statistical analysis was performed using the GraphPad Prism software (Graphpad Prism, RRID: SCR_002798). Statistical tests used are indicated in each figure legend, the asterisks on the figure indicate significant difference compared to the left-most bar.

Results

We previously reported the results of a genetic screen for suppressors of the dauer-constitutive (Daf-c) phenotype of the *daf-28(sa191)* mutant (Kulalert *et al.* 2017). Incomplete suppression of the Daf-c phenotype of the *daf-28(sa191)* mutant by *daf-3* and *daf-16* mutations (Malone *et al.* 1996; Li *et al.* 2003; Kulalert and Kim 2013) suggested that the identification of genetic suppressors of *daf-28(sa191)* might uncover additional novel pathways functioning in parallel to established signaling pathways activating the dauer developmental decision. Our prior characterization of the molecular mechanisms promoting dauer entry of the *daf-28(sa191)* mutant determined that activation of the Unfolded Protein Response and PEK-1 phosphorylation of eIF2α in the ASI neuron pair conferred the Daf-c phenotype (Kulalert and Kim 2013; Kulalert *et al.* 2017). We reported the isolation of multiple suppressor mutations in genes acting in this pathway downstream of UPR activation in the ASI neuron pair (Kulalert *et al.* 2017). We reasoned that we might also isolate suppressor mutations in novel pathways acting in parallel to this and previously characterized pathways leading to dauer formation. We recovered a strain carrying the *qd318* mutation from a genetic screen for suppressors of the Daf-c phenotype of the *daf-28(sa191)* mutant (Kulalert *et al.* 2017). Molecular characterization (described in Kulalert *et al.* 2017) of this strain revealed a P365S substitution mutation in the *mlk-1* gene encoding an MAPK kinase kinase. We sought to determine whether MLK-1 is also required for dauer entry in wild-type animals in the absence of the *daf-28(sa191)* mutation.

Induction of dauer formation under experimental conditions involves the addition of dauer pheromone, which is a combination of ascaroside molecules produced by *C. elegans* (Jeong *et al.* 2005; Butcher *et al.* 2007; Butcher *et al.* 2008; Pungaliya *et al.* 2009; Gallo and Riddle 2009), reduction of high-quality bacterial food *E. coli* OP50, and incubation at higher temperatures (Golden and Riddle 1984a, 1984b; Ailion and Thomas 2000; Neal *et al.* 2013). Figure 1A depicts an overview of the environmental conditions that affect the decision to enter dauer. We experimentally imposed environmental stressors of crowding, low food availability, and elevated ambient temperature in the laboratory, by exposing larvae to a combination of pheromone, heat-killed *E. coli* OP50, and incubation temperature of 25°C (Figure 1B). Under these conditions, we observed that >80% of wild-type larvae formed dauers (Figure 1C). In contrast, we observed that dauer formation was largely blocked in the *mlk-1(qd318)* mutant and a mutant carrying a deletion in the *mlk-1* gene, *mlk-1(km19)*.

MLK-1 has been previously characterized as acting upstream of the KGB-1 MAPK, which is homologous to the conserved JNK MAPK. MLK-1 phosphorylates the MAPK kinase MEK-1, a homolog of the MKK7 MAPKK, in the presence of the scaffold protein SHC-1, and MEK-1 phosphorylates and activates KGB-1 (Mizuno *et al.* 2004, 2008; Sakaguchi *et al.* 2004). All the kinase proteins in this pathway as well as the scaffold protein are essential for activation of KGB-1. The animals with loss-of-function mutations in genes encoding components of the KGB-1 pathway continued their reproductive growth, failing to enter dauer under these stressful conditions (Figure 1D). We determined that the KGB-1 MAPK is the only JNK MAPK required for dauer entry, as only *kgb-1* loss-of-function mutants (*km21* and *um3*) suppressed dauer entry, whereas the animals carrying mutations in the other two JNK homologs, *jnk-1(gk7)* and *kgb-2(gk361)*, were able to enter dauer similar to wild-type animals in the presence of the dauer inducing conditions (Figure 1E). The KGB-1 pathway was reported to have cross-talk with PMK-3 (p38 MAPK) pathway in axon regeneration where both the pathways are required (Nix *et al.* 2011), but we observed that the *pmk-3* loss-of-function mutant exhibited wild-type dauer entry (Figure 1E). Our data establish that the MLK-1-(SHC-1)-MEK-1-KGB-1 JNK MAPK pathway is required for dauer entry (Figure 1F).

To determine the tissue and cell types in which the KGB-1 pathway functions to promote dauer entry, we conducted tissue-specific rescue experiments of the *mek-1(qd375)* mutant using transgenes expressing the *mek-1* cDNA under the control of heterologous promoters. We fully rescued the Daf-d phenotype of the *mek-1(qd375)* mutant when expressing *mek-1* under its endogenous promoter and 3′UTR in an extrachromosomal array (Figure 2A). We observed that expression of *mek-1* in the nervous system of *mek-1(qd375)* mutant animals, under the control of the pan-neuronal promoter, *rab-3p*, resulted in rescue of the dauer formation phenotype, whereas expression of *mek-1* in the intestine or body wall muscles failed to rescue the Daf-d phenotype of the *mek-1(qd375)* mutant (Figure 2, B–D). In particular, we introduced expression of *mek-1* under the *bbs-1p* promoter, which directs expression in all ciliated neurons, and observed that expression in this specific subset of neurons

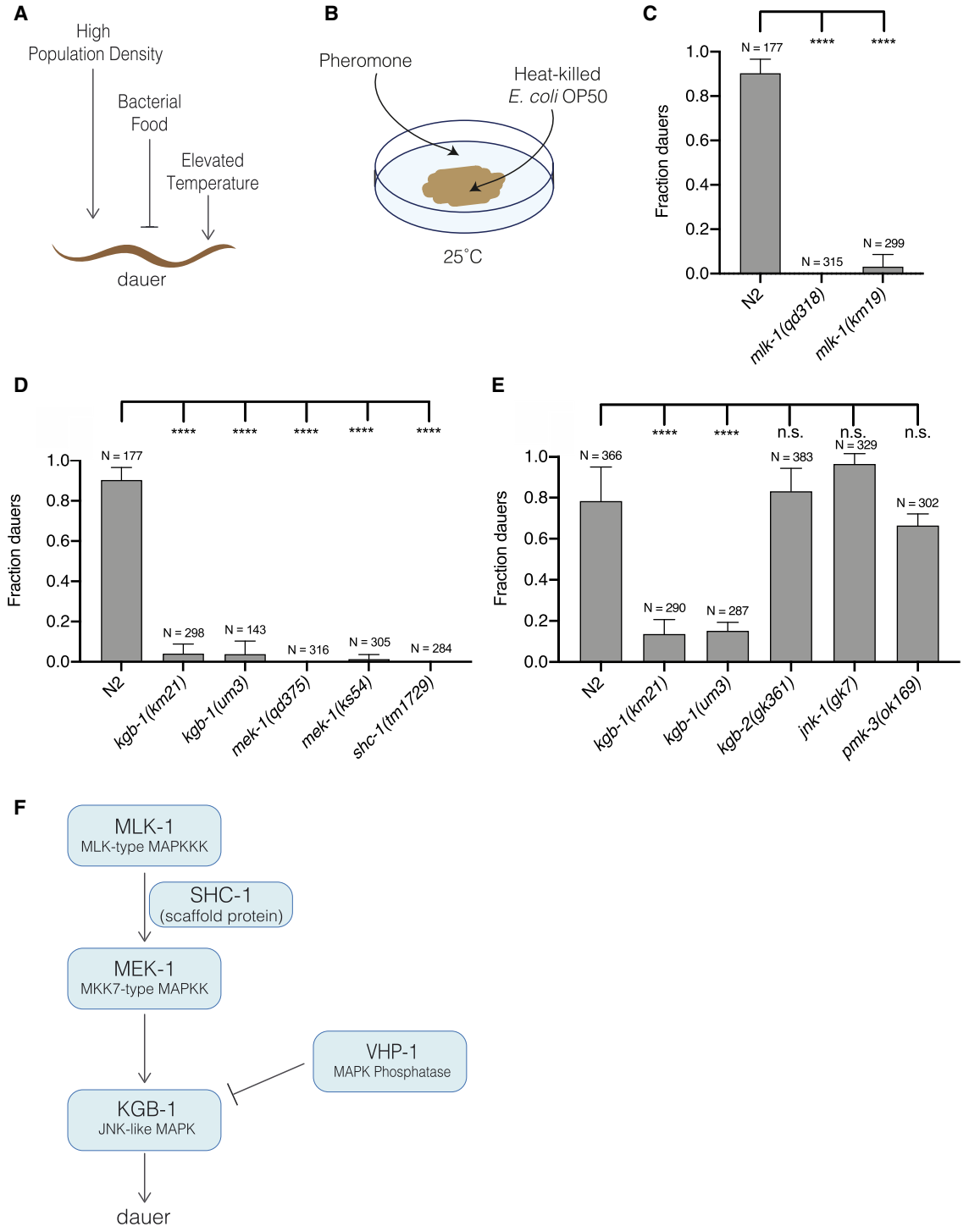

Figure 1 KGB-1 pathway activation is required for dauer entry caused by environmental stress. (A) Schematic depiction of environmental conditions that promote and suppress dauer formation. High population density and elevated temperature promote (shown by pointing arrows), and abundant food supply suppresses (shown by stopped line) dauer formation. (B) Schematic of dauer inducing conditions: a combination of pheromone, heat-killed *E. coli* OP50, and 25°C, applied to noble agar plates to emulate the environmental conditions promoting dauer formation depicted in (A). (C) Fraction of wild-type (N2) animals, and *mlk-1(qd318)* and *mlk-1(km19)* mutant animals entering dauer in the presence of dauer inducing conditions. Statistical analysis conducted with ordinary one-way ANOVA followed by Dunnett's multiple comparisons test. Plotted is mean + SD; N, total number of animals tested. (D) Fraction of wild-type (N2) animals, and *kgb-1(km21)*, *kgb-1(um3)*, *mek-1(qd375)*, *mek-1*(ks54), and *shc-1(tm1729)* mutant animals entering dauer in the presence of dauer-inducing conditions. Statistical analysis conducted with ordinary one-way ANOVA followed by Dunnett's multiple comparisons test. Plotted is mean + SD, N, = total number of animals tested. (E) Fraction of wild-type (N2) animals, and *kgb-1(km21)*, *kgb-1(um3)*, *kgb-2(gk361)*, *jnk-1(gk7)* and *pmk-3(ok169)* mutant animals entering dauer in the presence of dauer inducing conditions. Statistical analysis conducted with ordinary one-way ANOVA followed by Dunnett's multiple comparisons test. Plotted is mean + SD; N, total number of animals tested; n.s., not significant. (F) Schematic of KGB-1 pathway, a JNK-like MAPK pathway, composed of MLK-1 (MLK-type MAP3K), MEK-1 (MKK7-type MAP2K), SHC-1 (scaffold protein), KGB-1 (JNK-like MAPK) and VHP-1 (MAPK phosphatase).

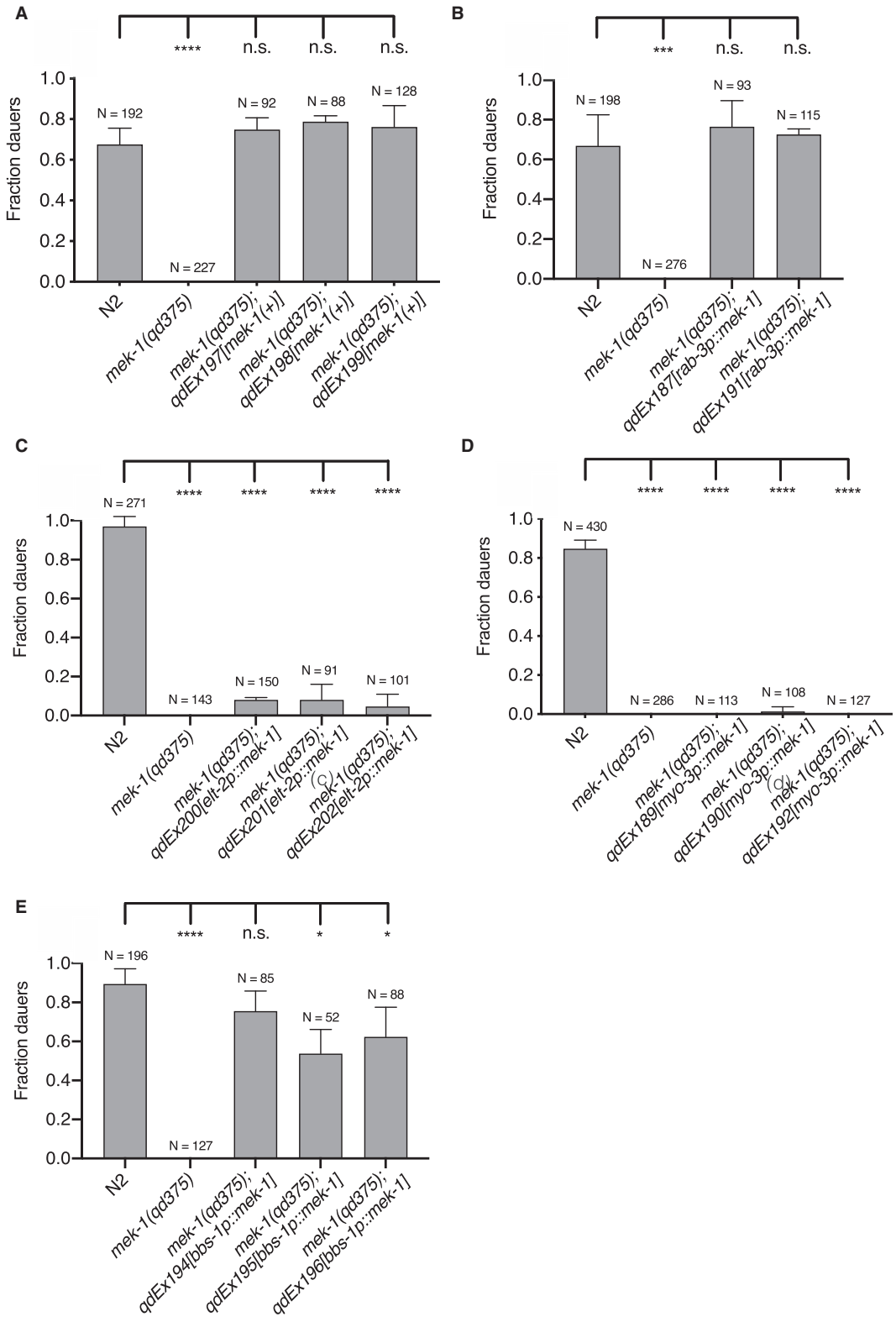

Figure 2 KGB-1 pathway acts in the chemosensory neurons to regulate dauer diapause. Fraction of wild-type (N2) animals, *mek-1(qd375)* mutant animals (non-sibling control) and *mek-1(qd375)* animals with extrachromosomal expression of (A) endogenous *mek-1* gene (B) *mek-1* gene under pan-neuronal promoter, *rab-3p* (C) *mek-1* gene under intestine-specific promoter, *elt-2p* (D) *mek-1* gene under body-wall muscle-specific promoter, *myo-3p* (E) *mek-1* gene under pan-ciliated neuron-specific promoter, *bbs-1p*, entering dauer in the presence of pheromone and heat-killed *E. coli* OP50 at 25°C. Statistical analysis conducted with ordinary one-way ANOVA followed by Dunnett's multiple comparisons test. Plotted is mean + SD; N, total number of animals tested; n.s., not significant.

rescued the Daf-d phenotype of *mek-1(qd375)* mutant animals (Figure 2E). Ciliated neurons encompass the chemosensory nervous system of *C. elegans*, and a number of specific sensory neurons have been implicated in roles in entry into, and exit from, dauer diapause (Albert *et al.* 1981; Bargmann and Horvitz 1991; Schackwitz *et al.* 1996; Ren *et al.* 1996; Li *et al.* 2003; Bargmann 2006; Ludewig and Schroeder 2013), but we were unable to further define specific neurons involved in dauer entry using neuronal cell type-specific rescue experiments. These data suggest either limitations of our experimental approach or the function of KGB-1 across multiple ciliated chemosensory neurons in dauer formation.

Having observed the effect of loss of KGB-1 signaling on blocking entry into dauer diapause, we sought to examine if increased KGB-1 signaling would confer the opposite phenotype of enhancing dauer formation. The VHP-1 MAPK phosphatase was previously characterized as a negative regulator of the KGB-1 MAPK, and diminished activity of VHP-1 resulted in hyperactivation of KGB-1 (Mizuno *et al.* 2004). A strain carrying a *vhp-1(km20)* deletion was previously noted to exhibit early larval lethality (Mizuno *et al.* 2004), but a viable *vhp-1* mutant carrying a nonsense mutation, *vhp-1(sa366)* has also been reported (Choy and Thomas 1999), and thus we examined this mutant for a dauer formation phenotype.

We examined wild-type and mutant larvae under 12 different sets of conditions derived from combinations of the presence or absence of pheromone, the presence of high-quality live bacterial food or poor quality heat-killed bacterial food, and three temperatures (25°C, 20°C, 16°C). The experimental data are presented in a 2 × 2 array, with each cell distinguished by the presence or absence of pheromone and whether larvae were exposed to live bacterial food or heat-killed bacterial food. Within each cell, the results of the three different incubation temperatures are presented. As we indicated above, optimal induction of dauer formation in wild-type animals was observed in the presence of dauer pheromone and heat-killed bacterial food at the elevated temperature of 25°C (Figure 3A). We did not observe dauer formation in the *vhp-1(sa366)* mutant in the absence of pheromone, even under conditions of bacterial food deprivation and elevated temperature, just as we observed for wild-type larvae. In the presence of pheromone and heat-killed food, we observed high-level dauer formation in *vhp-1(sa366)* larvae as was observed for wild-type animals. However, in contrast to what we observed for wild-type larvae, we detected equivalent high levels of dauer entry even at the lower temperatures of 20°C and 16°C under these conditions (Figure 3B). More dramatic differences were observed under conditions in the presence of pheromone and live bacterial food. In wild-type animals, the presence of live bacterial food largely suppressed dauer formation, but in *vhp-1(sa366)* animals, we observed marked dauer entry, equivalent to levels observed in the presence of heat-killed bacterial food.

We confirmed that *vhp-1(sa366)* is a hypomorphic allele by genetic analysis of trans-heterozygote animals using wild-type animals and the *vhp-1(km20)* null mutant (Figure 4, A–D). We confirmed that the absence of *kgb-1* suppresses dauer formation in the *vhp-1(sa366)* mutant animals. We also confirmed that dauer formation in the *vhp-1(sa366)* mutant was suppressed by mutation in the KGB-1 pathway, specifically a mutation in the *mek-1* gene encoding the MAPKK MEK-1 that phosphorylates KGB-1 (Figure 4, E and F). In the absence of phosphorylation of KGB-1, reduction of function of the VHP-1 phosphatase would not be expected to affect KGB-1 activity.

These data suggest that increased activity of the KGB-1 pathway in the *vhp-1(sa366)* mutant can substitute for the requirement for diminished bacterial food availability and elevated temperature in the induction of dauer formation, whereas the requirement for pheromone is unaffected by increased KGB-1 activity. We next sought to define the genetic interactions among KGB-1 signaling and established pathways involved in the dauer developmental decision. We determined that the enhanced dauer entry phenotype of *vhp-1(sa366)* mutant larvae was suppressed by *daf-12* (Figure 5, A and B), as is the case with all known dauer-constitutive mutants (Vowels and Thomas 1992). We observed that the *daf-16(mu86); vhp-1(sa366)* mutant in the presence of pheromone resulted in the formation of partial dauers, regardless of whether live or heat-killed bacterial food was present (Figure 5, C and D). Partial dauer formation was also observed in double mutants involving *daf-16* and dauer-constitutive mutants, including *daf-28(sa191)* (Vowels and Thomas 1992; Malone *et al.* 1996), but not observed in *daf-2; daf-16* double mutants. The observation of partial dauers in the *daf-16(mu86); vhp-1(sa366)* mutant animals suggests that the KGB-1 signaling can activate the developmental decision to commit to dauer entry and partially proceed independent of DAF-16, but that the full execution of dauer program requires DAF-16 activity.

We observed that *daf-3(e1376); vhp-1(sa366)* mutants did not enter dauer in the presence of pheromone (Figure 6, A and B). One interpretation of this observation was that KGB-1 signaling might function upstream of DAF-7-DAF-3 signaling. Alternatively, because pheromone is required for *vhp-1(sa366)*-enhanced dauer formation, we considered the possibility that KGB-1 signaling might function in parallel with DAF-7-DAF-3 signaling, with the *daf-3* mutation attenuating the effect of pheromone. Indeed, *daf-7* mutants exhibit a dauer-constitutive phenotype in the absence of pheromone, and pheromone downregulates *daf-7* expression in the ASI sensory neurons (Thomas *et al.* 1993; Ren *et al.* 1996; Schackwitz *et al.* 1996). To distinguish between these possibilities, we utilized a previously described reporter of DAF-3 activity, *cuIs5* (Thatcher *et al.* 1999; Reiner *et al.* 2008). This reporter consists of *myo-2* promoter, preceded by tandem copies of C183 portion of C-subelement, driving GFP expression in the pharynx. DAF-3 specifically recognizes and binds to C183 causing a suppression of GFP expression when it is not inhibited by DAF-7 (Figure 6C). As expected and has been reported, in the *daf-7* mutant background, DAF-3 reporter activity is diminished. The presence of pheromone also decreased DAF-3 reporter activity relative to conditions in the absence of pheromone although no difference was observed in the *daf-7* mutant, consistent with the *daf-7* mutant mimicking conditions of pheromone presence. If *vhp-1(sa366)* promoted dauer entry by modulating DAF-3 activity, we would expect DAF-3 reporter activity to be similarly diminished in the *vhp-1(sa366)* background in the presence of pheromone. We observed that DAF-3 reporter activity was not affected by the *vhp-1(sa366)* mutation (Figure 6D). These data suggest that the *vhp-1(sa366)* mutation and corresponding KGB-1 activity function in parallel to TGF-β signaling to promote dauer entry, and indicate that pheromone may act in part through modulation of the DAF-3-dependent signaling pathway.

Discussion

Dauer entry represents an integrated organismal response to environmental stress during development. Stress-activated MAPK signaling pathway have evolutionarily conserved roles in a wide range of stress responses in diverse species, and the KGB-1 JNK MAPK pathway has been implicated in the *C. elegans* response to

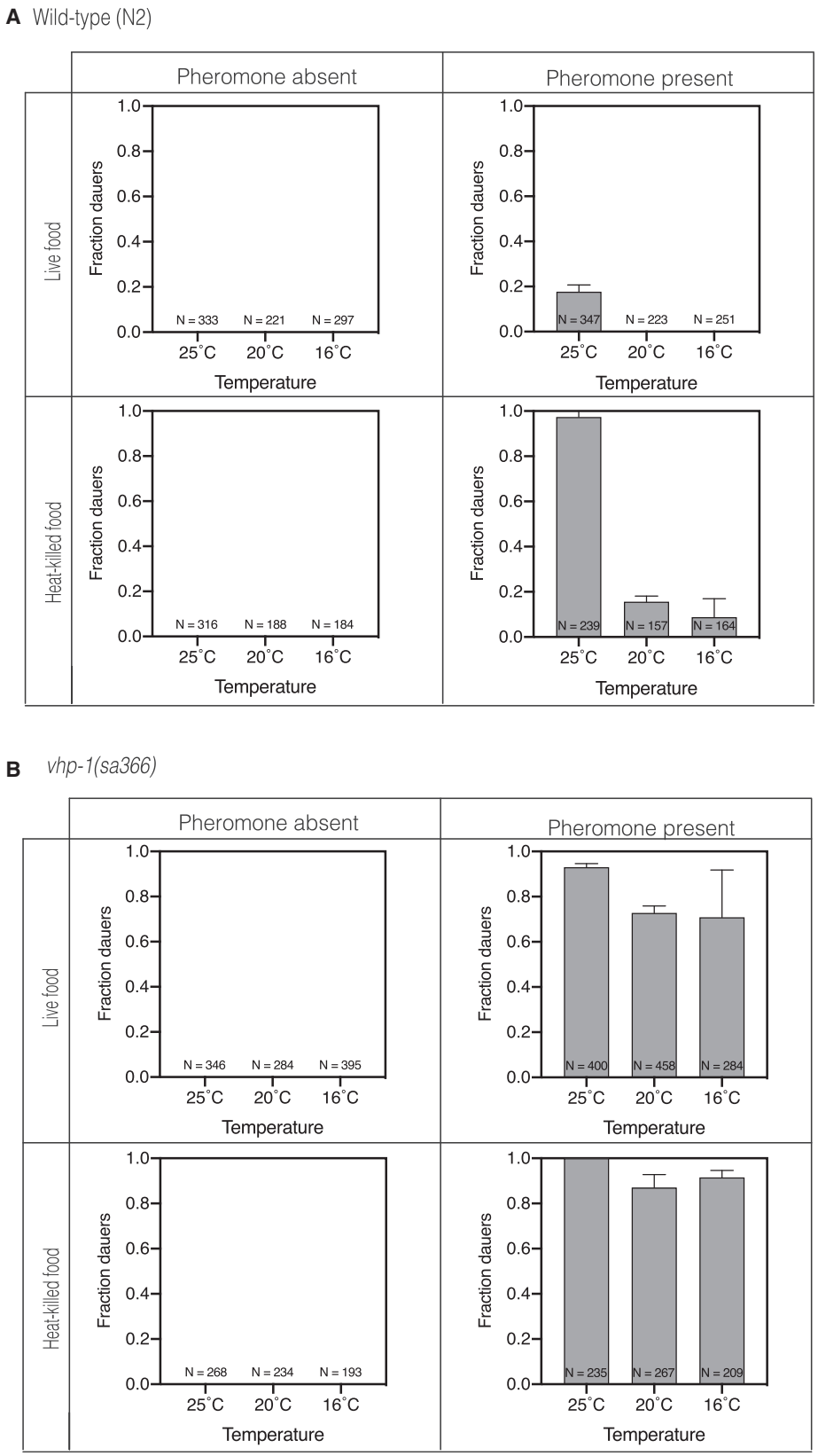

Figure 3 Increased activation of the KGB-1 pathway in the *vhp-1* mutant leads to constitutive dauer formation in the presence of pheromone. Fraction of (A) wild-type animals (B) *vhp-1(sa366)* mutant animals entering dauer under various combinations of dauer inducing conditions. The first row shows fraction dauers in the presence of live *E. coli* OP50 and the second row shows fraction dauers in the presence of heat-killed *E. coli* OP50. The first column shows fraction dauers in the absence of pheromone and the second column shows fraction dauers in the presence of pheromone. Each graph in the four panels shows fraction dauers at 25C, 20°C and 16°C, respectively. Plotted is mean + SD; N, total number of animals tested.

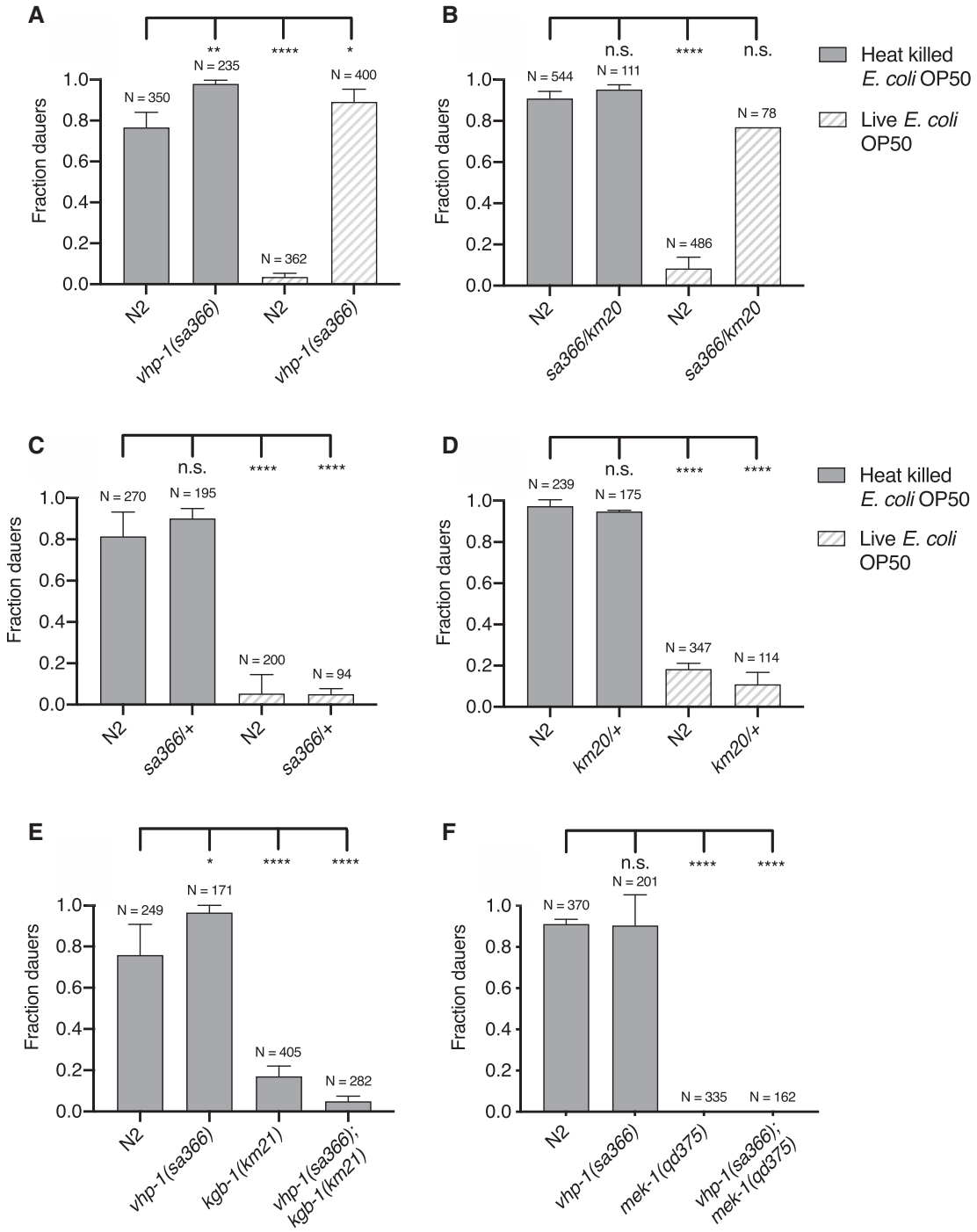

Figure 4 Dauer formation of *vhp-1(sa366)* mutant animals is due to hyperactivation of KGB-1 pathway. (A–D) Fraction of wild-type (N2) animals and (A) *vhp-1(sa366)* homozygous mutant animals (B) *vhp-1(sa366/km20)* heterozygous mutant animals (C) *vhp-1(sa366/+)* heterozygous mutant animals (D) *vhp-1(km20/+)* heterozygous mutant animals, entering dauer in the presence of pheromone, 25°C and either heat-killed (solid bars) or live (patterned bars) *E. coli* OP50. Statistical analysis conducted with ordinary one-way ANOVA followed by Dunnett's multiple comparisons test. Plotted is mean + SD, N = total number of animals tested, n.s. = not significant. (E, F) Fraction of wild-type (N2) animals, *vhp-1(sa366)*, (E) *kgb-1(km21)* and *vhp-1(sa366); kgb-1(km21)*, (F) *mek-1(qd375)* and *vhp-1(sa366); mek-1(qd375)* mutant animals, entering dauer in the presence of pheromone, 25°C and heat-killed *E. coli* OP50. Statistical analysis conducted with ordinary one-way ANOVA followed by Dunnett's multiple comparisons test. Plotted is mean + SD; N, total number of animals tested; n.s., not significant.

multiple stressors, including heavy metals (Koga *et al.* 2000; Mizuno *et al.* 2004), the ER toxin tunicamycin (Mizuno *et al.* 2008), and food deprivation in the context of lifespan extension through intermittent fasting (Uno *et al.* 2013). KGB-1 is also required for resistance to pathogenic bacteria (Kim *et al.* 2004) and pore-forming toxins (Huffman *et al.* 2004). Here, our data suggest a role for KGB-1 signaling in the dauer developmental decision, with increased KGB-1 signaling in the *vhp-1* mutant enabling dauer formation independent of bacterial food availability and temperature. Previous studies establishing an age-dependent role of

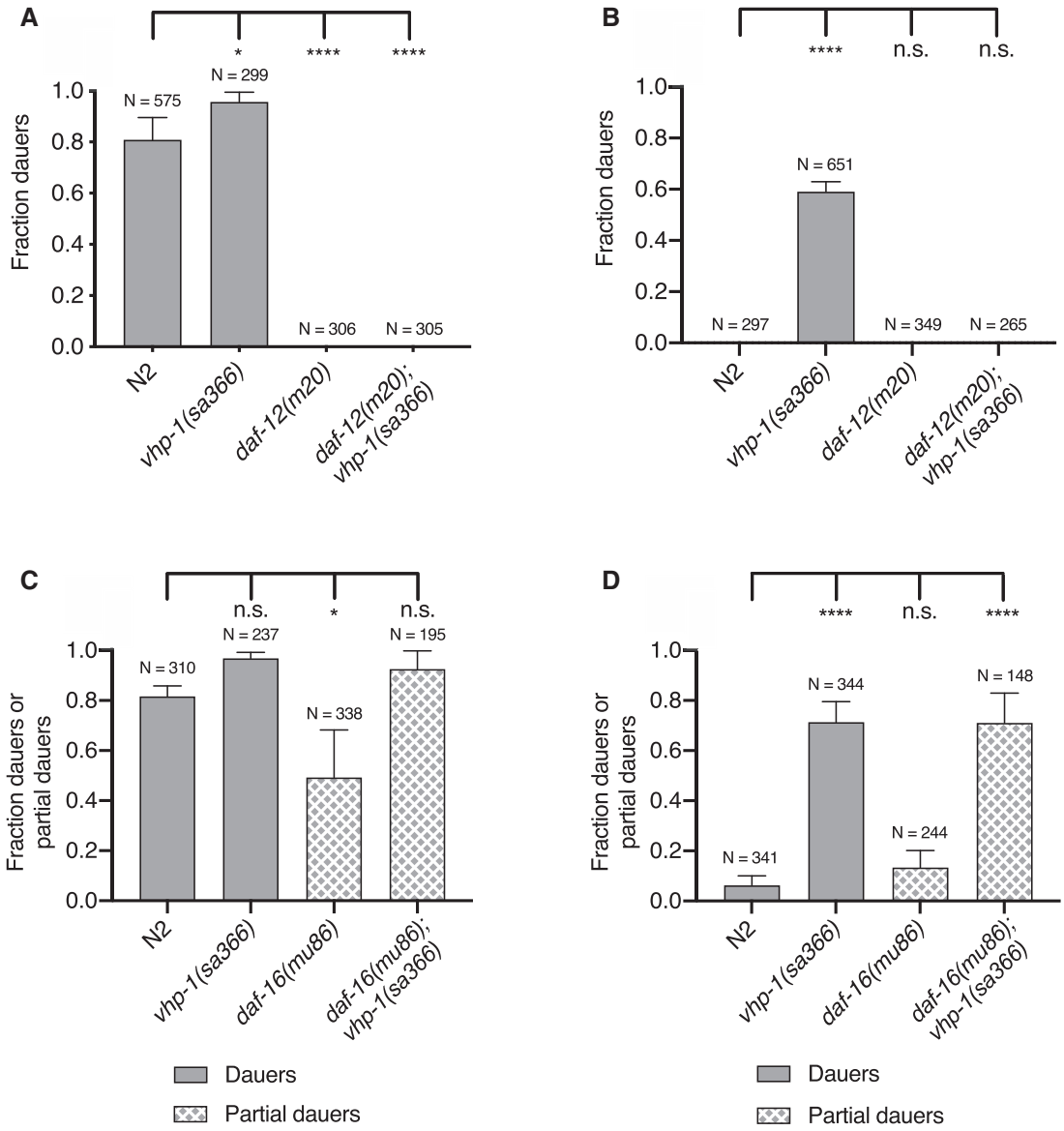

Figure 5 KGB-1 pathway functions upstream of the steroidal hormone pathway and in parallel to the insulin signaling pathway. (A, B) Fraction of wild-type (N2) animals and *vhp-1(sa366)*, *daf-12(m20)* and *daf-12(m20); vhp-1(sa366)* mutant animals entering dauer in the presence of pheromone, 25°C and (A) heat-killed *E. coli* OP50 (B) live *E. coli* OP50. Statistical analysis conducted with ordinary one-way ANOVA followed by Dunnett's multiple comparisons test. Plotted is mean + SD; N, total number of animals tested; n.s., not significant. (C, D) Fraction of wild-type (N2) animals and *vhp-1(sa366)*, *daf-16(mu86)* and *daf-16(mu86); vhp-1(sa366)* mutant animals entering dauer in the presence of pheromone, 25°C and (C) heat-killed *E. coli* OP50 (D) live *E. coli* OP50. Statistical analysis conducted with ordinary one-way ANOVA followed by Dunnett's multiple comparisons test. Plotted is mean + SD; N, total number of animals tested; n.s., not significant.

KGB-1 pathway described interaction with insulin signaling pathway, specifically DAF-16 (Twumasi-Boateng et al. 2012; Liu *et al.* 2018). Our epistasis analysis suggests that the KGB-1 pathway functions in parallel to insulin signaling in the decision to enter dauer diapause, but that full execution of the dauer program requires DAF-16 as indicated by the formation of incomplete, or partial dauers in the absence of DAF-16.

Early studies established that the ratio of pheromone to bacterial food is more important than the absolute concentration *per se* in regulating dauer entry. Using serial dilutions of both pheromone and food concentrations, Riddle and colleagues showed that dauer phenotype is dependent on the relative concentration of the signals (Golden and Riddle 1982, 1984a). Higher pheromone concentration induces a greater fraction of the population to enter dauer but this effect saturates at a fraction dependent on the total amount of bacterial food present (Golden and Riddle 1984b). Similarly, increases in temperature enhance dauer entry in the presence of a constant pheromone to food ratio (Golden and Riddle 1984b, 1984c). Our results suggest a role of the KGB-1 pathway in the interpretation of the pheromone to food ratio in the dauer developmental decision. Whereas the prior identification of dauer-defective mutants and, correspondingly, signaling pathways that promote dauer formation have largely been in the experimental context of suppression of Daf-c mutations, recent studies have focused on the genetic characterization of dauer entry in wild-type larvae in response to environmental cues. Of note, mutants of Rictor/TORC2 exhibit high temperature (27°C) induced dauer entry, in a manner that was also not affected by

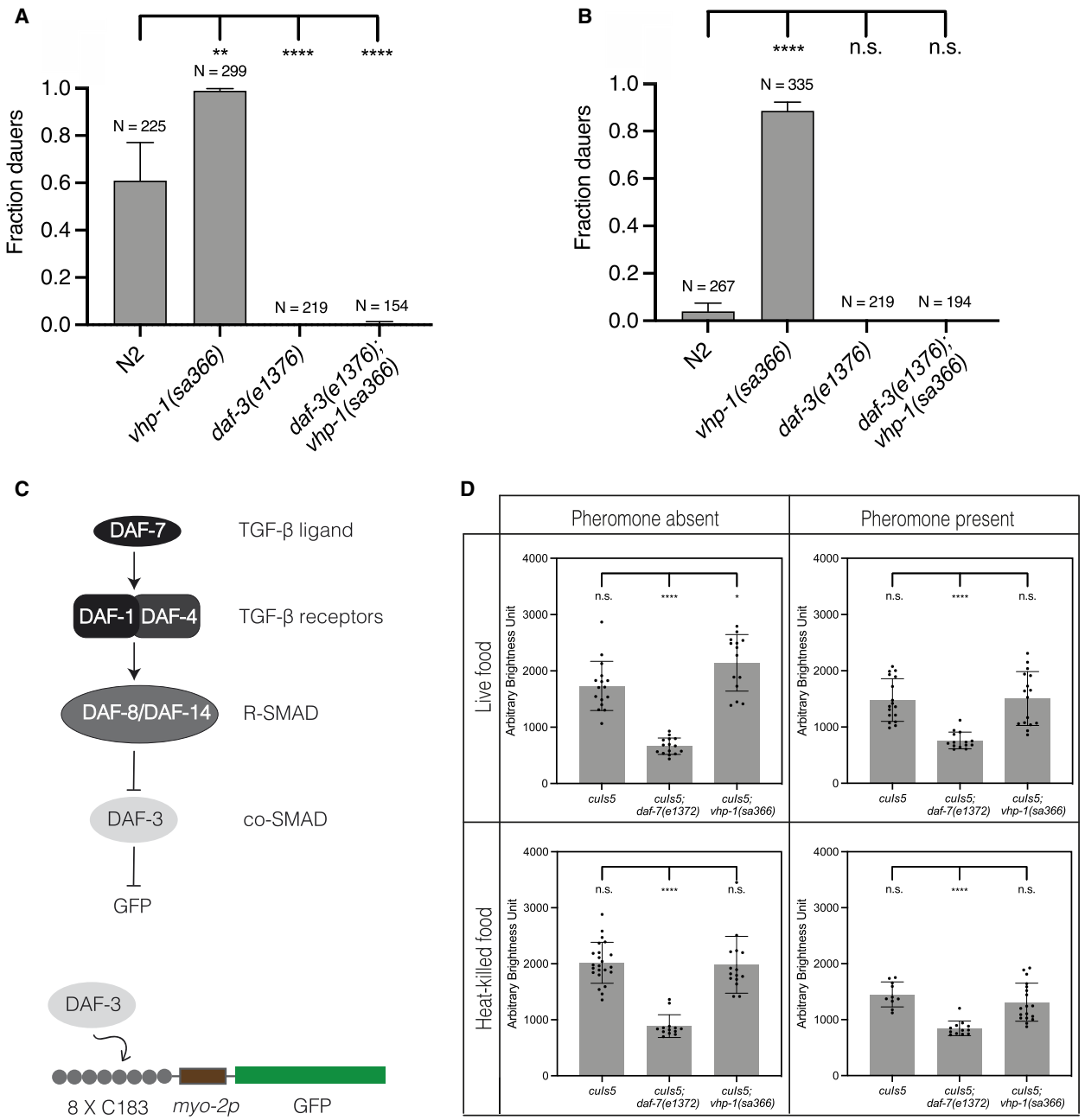

Figure 6 KGB-1 pathway functions in parallel to TGF-β signaling pathway in regulation of dauer diapause. (A, B) Fraction of wild-type (N2) animals, *vhp-1(sa366)*, *daf-3(e1376)* and *daf-3(e1376); vhp-1(sa366)* mutant animals entering dauer in the presence of pheromone, 25°C and (A) heat-killed *E. coli* OP50 (B) live *E. coli* OP50. Statistical analysis conducted with ordinary one-way ANOVA followed by Dunnett's multiple comparisons test. Plotted is mean + SD, *N* = total number of animals tested, n.s. = not significant. (C) Overview of TGF-β signaling pathway and schematic of *culs5*—DAF-3 reporter transgene. (D) Quantification of GFP expression from DAF-3 reporter (*culs5*). Each graph in the four panels shows GFP expression in wild-type background, *daf-7(e1372)* and *vhp-1(sa366)* mutant backgrounds, respectively. The first row shows fraction dauers in the presence of live *E. coli* OP50 and the second row shows fraction dauers in the presence of heat-killed *E. coli* OP50. The first column shows fraction dauers in the absence of pheromone and the second column shows fraction dauers in the presence of pheromone. Plotted is mean + SD, each dot represents an animal; n.s., not significant.

bacterial food quality, and the Rictor/TORC2 pathway was implicated in relaying food-sensing information from the intestine to the nervous system (O'Donnell *et al.* 2018). Whereas *rict-1* mutants modulated neuronal expression of *daf-7*, our data suggest that KGB-1 signaling mediates food sensitivity in parallel to the DAF-7/TGF-β signaling pathway.

Our epistasis analysis suggests that KGB-1 signaling functions in parallel to the insulin/DAF-16 and DAF-7/TGF-β signaling pathways are also consistent with the KGB-1 pathway functioning downstream of nutrient and/or temperature inputs into the dauer decision, independent of pheromone. Pheromone has been shown to modulate the expression of DAF-7 (Ren *et al.* 1996; Schackwitz *et al.* 1996) and insulin ligands of DAF-2 (Li *et al.* 2003; Cornils *et al.* 2011; Wong *et al.* 2020) consistent with a role for the insulin/DAF-16 and DAF-7/TGF-β signaling pathways downstream of pheromone input, and unlike wild-type animals or *vhp-1* mutant animals, dauer-constitutive mutants of the insulin/DAF-16 and DAF-7/TGF-β signaling pathways can form dauer independent of the presence of pheromone. Our study suggests that the activity of a conserved stress-activated KGB-1 signaling in the sensory nervous system is

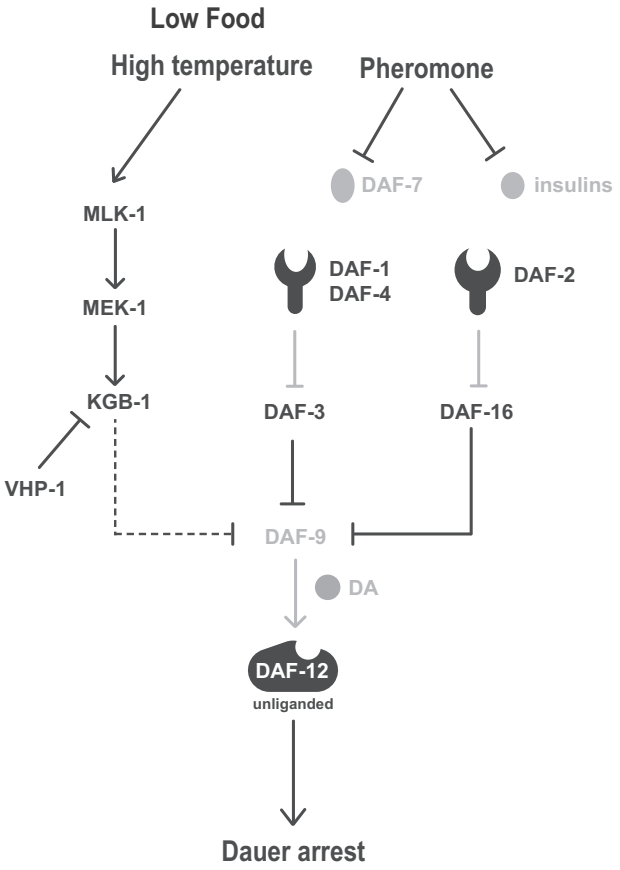

Figure 7 Model figure depicting KGB-1 pathway functioning parallel to TGF-β and insulin signaling pathways in response to stress conditions of diminished food and elevated temperature to regulate dauer formation. Dashed line depicts tentative placement of KGB-1 pathway upstream of DAF-9. DA, dafachronic acids.

required for the dauer developmental decision in response to diminished food availability as well as increased temperature, activating dauer entry in the presence of pheromone in parallel to established neuroendocrine pathways involved in the regulation of dauer formation (Figure 7).

Data availability

Strains are available upon request. The authors state that all data necessary for confirming the conclusions presented in the article are represented fully within the article.

Acknowledgments

The authors thank the Caenorhabditis Genetics Center, which is funded by NIH Office of Research Infrastructure Programs (P40 OD010440), for providing strains. They also thank members of the Kim lab for helpful conversations and feedback on the manuscript and figures.

Funding

This work is supported by NIGMS grants R01GM084477 and R35GM141794 to D.H.K. and R35GM131877 to F.C.S.

Conflict of interest

The authors declare that there is no conflict of interest.

Literature cited

Ailion M, Thomas JH. 2000. Dauer formation induced by high temperatures in *Caenorhabditis elegans*. Genetics. 156:1047–1067.

Albert PS, Brown SJ, Riddle DL. 1981. Sensory control of dauer larva formation in *Caenorhabditis elegans*. J Comp Neurol. 198:435–451.

Bargmann CI, Horvitz HR. 1991. Control of larval development by chemosensory neurons in *Caenorhabditis elegans*. Science. 251: 1243–1246.

Bargmann CI. 2006. Chemosensation in *C. elegans* (October 25, 2006). In: The *C. elegans* Research CommunityWormBook, editor. WormBook. doi/10.1895/wormbook.1.123.1. http://www.wormbook.org.

Baugh LR, Hu PJ. 2020. Starvation responses throughout the *Caenorhabditis elegans* life cycle. Genetics. 216:837–878.

Butcher RA, Fujita M, Schroeder FC, Clardy J. 2007. Small-molecule pheromones that control dauer development in *Caenorhabditis elegans*. Nat Chem Biol. 3:420–422.

Butcher RA, Ragains JR, Kim E, Clardy J. 2008. A potent dauer pheromone component in *Caenorhabditis elegans* that acts synergistically with other components. Proc Natl Acad Sci U S A. 105: 14288–14292.

Cassada RC, Russell RL. 1975. The dauerlarva, a post-embryonic developmental variant of the nematode *Caenorhabditis elegans*. Dev Biol. 46:326–342.

Choy RK, Thomas JH. 1999. Fluoxetine-resistant mutants in *C. elegans* define a novel family of transmembrane proteins. Mol Cell. 4:143–152.

Cornils A, Gloeck M, Chen Z, Zhang Y, Alcedo J. 2011. Specific insulin-like peptides encode sensory information to regulate distinct developmental processes. Development. 138:1183–1193.

Fielenbach N, Antebi A. 2008. *C. elegans* dauer formation and the molecular basis of plasticity. Genes Dev. 22:2149–2165.

Gallo M, Riddle DL. 2009. Effects of a *Caenorhabditis elegans* dauer pheromone ascaroside on physiology and signal transduction pathways. J Chem Ecol. 35:272–279.

Golden JW, Riddle DL. 1982. A pheromone influences larval development in the nematode *Caenorhabditis elegans*. Science. 218: 578–580.

Golden JW, Riddle DL. 1984a. A *Caenorhabditis elegans* dauer-inducing pheromone and an antagonistic component of the food supply. J Chem Ecol. 10:1265–1280.

Golden JW, Riddle DL. 1984b. A pheromone-induced developmental switch in *Caenorhabditis elegans*: temperature-sensitive mutants reveal a wild-type temperature-dependent process. Proc Natl Acad Sci U S A. 81:819–823.

Golden JW, Riddle DL. 1984c. The *Caenorhabditis elegans* dauer larva: developmental effects of pheromone, food, and temperature. Dev Biol. 102:368–378.

Hu PJ. 2007. Dauer (August 8, 2007). In: The *C. elegans* Research Community WormBook, editor. WormBook. doi/10.1895/wormbook.1.144.1. http://www.wormbook.org.

Huffman DL, Abrami L, Sasik R, Corbeil J, van der Goot FG, *et al.* 2004. Mitogen-activated protein kinase pathways defend against bacterial pore-forming toxins. Proc Natl Acad Sci U S A. 101: 10995–11000.

Jeong PY, Jung M, Yim YH, Kim H, Park M, *et al.* 2005. Chemical structure and biological activity of the *Caenorhabditis elegans* dauer-inducing pheromone. Nature. 433:541–545.

Kaul TK, Rodrigues PR, Ogungbe IV, Kapahi P, Gill MS. 2014. Bacterial fatty acids enhance recovery from the dauer larva in *Caenorhabditis elegans*. PLoS One. 9:e86979.

Kim DH, Liberati NT, Mizuno T, Inoue H, Hisamoto N, *et al.* 2004. Integration of *Caenorhabditis elegans* MAPK pathways mediating immunity and stress resistance by MEK-1 MAPK kinase and VHP-1 MAPK phosphatase. Proc Natl Acad Sci U S A. 101: 10990–10994.

Kim K, Sato K, Shibuya M, Zeiger DM, Butcher RA, *et al.* 2009. Two chemoreceptors mediate developmental effects of dauer pheromone in *C. elegans*. Science. 326:994–998.

Koga M, Zwaal R, Guan KL, Avery L, Ohshima Y. 2000. A *Caenorhabditis elegans* MAP kinase kinase, MEK-1, is involved in stress responses. EMBO J. 19:5148–5156.

Kulalert W, Kim DH. 2013. The unfolded protein response in a pair of sensory neurons promotes entry of *C. elegans* into dauer diapause. Curr Biol. 23:2540–2545.

Kulalert W, Sadeeshkumar H, Zhang YK, Schroeder FC, Kim DH. 2017. Molecular determinants of the regulation of development and metabolism by neuronal eIF2α phosphorylation in *Caenorhabditis elegans*. Genetics. 206:251–263.

Larsen PL, Albert PS, Riddle DL. 1995. Genes that regulate both development and longevity in *Caenorhabditis elegans*. Genetics. 139: 1567–1583.

Li W, Kennedy SG, Ruvkun G. 2003. *daf-28* encodes a *C. elegans* insulin superfamily member that is regulated by environmental cues and acts in the DAF-2 signaling pathway. Genes Dev. 17:844–858.

Liu L, Ruediger C, Shapira M. 2018. Integration of stress signaling in *Caenorhabditis elegans* through cell-nonautonomous contributions of the JNK homolog KGB-1. Genetics. 210:1317–1328.

Ludewig AH, Schroeder FC. 2013. Ascaroside signaling in *C. elegans* (January 18, 2013). In: The *C. elegans* Research Community WormBook, editor. WormBook. doi/10.1895/wormbook.1.155.1. http://www.wormbook.org.

Malone EA, Inoue T, Thomas JH. 1996. Genetic analysis of the roles of *daf-28* and *age-1* in regulating *Caenorhabditis elegans* Dauer formation. Genetics. 143:1193–1205.

McGrath PT, Xu Y, Ailion M, Garrison JL, Butcher RA, *et al.* 2011. Parallel evolution of domesticated *Caenorhabditis* species targets pheromone receptor genes. Nature. 477:321–325.

Mizuno T, Fujiki K, Sasakawa A, Hisamoto N, Matsumoto K. 2008. Role of the *Caenorhabditis elegans* Shc adaptor protein in the c-Jun N-terminal kinase signaling pathway. Mol Cell Biol. 28: 7041–7049.

Mizuno T, Hisamoto N, Terada T, Kondo T, Adachi M, *et al.* 2004. The *Caenorhabditis elegans* MAPK phosphatase VHP-1 mediates a novel JNK-like signaling pathway in stress response. EMBO. 23: 2226–2234.

Neal SJ, Kim K, Sengupta P. 2013. Quantitative assessment of pheromone-induced dauer formation in Caenorhabditis elegans. In: Touhara K, editor. *Pheromone Signaling*. Totowa, NJ: Humana Press. p. 273–283.

Neal SJ, Takeishi A, O'Donnell MP, Park J, Hong M, *et al.* 2015. Feeding state-dependent regulation of developmental plasticity via CaMKI and neuroendocrine signaling. Elife. 4:e10110.

Nika L, Gibson T, Konkus R, Karp X. 2016. Fluorescent beads are a versatile tool for staging *Caenorhabditis elegans* in different life histories. G3. G3 (Bethesda). 6:1923–1933.

Nix P, Hisamoto N, Matsumoto K, Bastiani M. 2011. Axon regeneration requires coordinate activation of p38 and JNK MAPK pathways. Proc Natl Acad Sci U S A. 108:10738–10743.

O'Donnell MP, Chao PH, Kammenga JE, Sengupta P. 2018. Rictor/TORC2 mediates gut-to-brain signaling in the regulation of phenotypic plasticity in *C. elegans*. PLoS Genet. 14:e1007213.

Ogg S, Paradis S, Gottlieb S, Patterson GI, Lee L, *et al.* 1997. The Fork head transcription factor DAF-16 transduces insulin-like metabolic and longevity signals in *C. elegans*. Nature. 389:994–999.

Park D, O'Doherty I, Somvanshi RK, Bethke A, Schroeder FC, *et al.* 2012. Interaction of structure-specific and promiscuous G-protein–coupled receptors mediates small-molecule signaling in *Caenorhabditis elegans*. Proc Natl Acad Sci U S A. 109:9917–9922.

Pungaliya C, Srinivasan J, Fox BW, Malik RU, Ludewig AH, *et al.* 2009. A shortcut to identifying small molecule signals that regulate behavior and development in *Caenorhabditis elegans*. Proc Natl Acad Sci U S A. 106:7708–7713.

Reiner DJ, Ailion M, Thomas JH, Meyer BJ. 2008. *C. elegans* anaplastic lymphoma kinase ortholog SCD-2 controls dauer formation by modulating TGF-β signaling. Curr Biol. 18:1101–1109.

Ren P, Lim CS, Johnsen R, Albert PS, Pilgrim D, *et al.* 1996. Control of *C. elegans* larval development by neuronal expression of a TGF-β homolog. Science. 274:1389–1391.

Riddle DL, Albert PS. 1997. Genetic and environmental regulation of dauer larva development. In: DL Riddle, T Blumenthal, BJ Meyer, JR Priess, editors. C. elegans II. Plainview, NY: Cold Spring Harbor Laboratory Press. p. 739–768.

Sakaguchi A, Matsumoto K, Hisamoto N. 2004. Roles of MAP kinase cascades in *Caenorhabditis elegans*. J Biochem. 136:7–11.

Schackwitz WS, Inoue T, Thomas JH. 1996. Chemosensory neurons function in parallel to mediate a pheromone response in *C. elegans*. Neuron. 17:719–728.

Schindelin J, Arganda-Carreras I, Frise E, Kaynig V, Longair M, *et al.* 2012. Fiji: an open-source platform for biological-image analysis. Nat Methods. 9:676–682.

Thatcher JD, Haun C, Okkema PG. 1999. The DAF-3 Smad binds DNA and represses gene expression in the *Caenorhabditis elegans* pharynx. Development. 126:97–107.

Thomas JH, Birnby DA, Vowels JJ. 1993. Evidence for parallel processing of sensory information controlling dauer formation in *Caenorhabditis elegans*. Genetics. 134:1105–1117.

Twumasi-Boateng K, Wang TW, Tsai L, Lee KH, Salehpour A, *et al.* 2012. An age-dependent reversal in the protective capacities of JNK signaling shortens *Caenorhabditis elegans* lifespan. Aging Cell. 11:659–667.

Uno M, Honjoh S, Matsuda M, Hoshikawa H, Kishimoto S, *et al.* 2013. A fasting-responsive signaling pathway that extends life span in *C. elegans*. Cell Rep. 3:79–91.

Vowels JJ, Thomas JH. 1992. Genetic analysis of chemosensory control of dauer formation in *Caenorhabditis elegans*. Genetics. 130: 105–123.

Wong SS, Yu J, Schroeder FC, Kim DH. 2020. Population density modulates the duration of reproduction of *C. elegans*. Curr Biol. 30: 2602–2607.

Communicating editor: E. Hallem